Russian Chemical Bulletin, International Edition, Vol. 50, No. 3, pp. 488—493, March, 2001

Synthesis and magnetic properties of liquid crystalline lanthanide complexes with alkylsulfate counterions

L. V. Malykhina,[a] A. V. Prosvirin,[b] W. Haase,[c] and Yu. G. Galyametdinov[a,b]★

[a]Kazan State Technological University,
68 ul. K. Marksa, 420015 Kazan, Russian Federation.
[b]E. K. Zavoisky Kazan Physical-Technical Institute of the Russian Academy of Sciences,
10/7 ul. Sibirsky Trakt, 420029 Kazan, Russian Federation.
E-mail: galyametdinov@sci.kcn.ru
[c]Technische Universität Darmstadt, Institute für physikalische Chemie I,
20 Petersenstr., D-64257, Darmstadt, Germany

The reaction of Schiff's base L with lanthanide alkylsulfates affords liquid crystalline complexes with the general formula $L_3Ln(C_nH_{2n+1}OSO_3)_3$. The liquid crystalline structure and magnetic properties are studied by polarization thermal microscopy, differential scanning calorimetry, X-ray diffraction, and measurement of magnetic susceptibility. The temperatures of the existence of the mesophase and magnetic anisotropy of the complexes with the same lanthanide depend on the chain length of the alkyl fragment in the sulfate anion.

Key words: metallomesogens, lanthanides, structure, magnetic susceptibility.

The most works on liquid crystalline metal complexes are devoted to methods of their synthesis.[1—3] The physicochemical (dielectric[4] and optical[5]) properties of this class of liquid crystals have been reported recently. The introduction of lanthanides into mesogenic substances allowed the creation of liquid crystalline materials with a high magnetic anisotropy.[6—7] For this reason we hope that thermostable and low-viscosity liquid crystals, which could easily be controlled by weak magnetic fields and undoubtedly find use in the magnetooptics of liquid crystals, exist among these compounds. Thermotropic metallomesogens have a substantial disadvantage: high (often >200 °C) temperatures of the existence of their mesophase resulting in the decomposition of the compounds in the mesophase or during the phase transition to the state of an isotropic liquid. The study of the liquid crystalline lanthanides L_3LnX_3 (Ln = Tb, Er; X = Cl^-, NO_3^-;

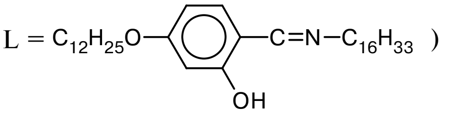

showed that the temperatures of phase transitions in them can decrease by 30—40 °C when the Cl^- counterion is replaced by NO_3^- remaining, however, rather high.[8—9] The temperature of their isotropization is ~150—160 °C. The lanthanide complexes containing the dodecylsulfate anion as a counterion were prepared later.[10] They possess much lower (as compared to the nitrates and chlorides) temperatures of phase transitions.[10]

In this work, we studied the influence of the alkyl chain in the alkylsulfate $C_nH_{2n+1}OSO_3$ counterion on the temperature of phase transitions and magnetic properties of the lanthanide complexes with Schiff's bases.

Results and Discussion

The L_3LnX_3 complexes were synthesized by the reaction of sodium alkylsulfate with $LnCl_3$ followed by the interaction of equimolar amounts of the corresponding ligand and lanthanide alkylsulfate in ethanol (Scheme 1).

Scheme 1

$$LnCl_3 + 3\ ROSO_3Na \longrightarrow Ln(R—OSO_3)_3 + 3\ NaCl, \quad (1)$$

where R = C_nH_{2n+1}, n = 2—10, 12, 13, 15, 18, 19

$$3\ L + Ln(R—OSO_3)_3 \longrightarrow L_3Ln(R—OSO_3)_3. \quad (2)$$

The liquid crystalline properties and type of the mesophases of the synthesized compounds were studied by polarization thermal microscopy, differential scanning calorimetry (DSC) (Fig. 1), and X-ray diffraction (XRD).

The influence of the alkyl chain length in the counterion on the temperatures of transitions from the crystalline (Cr) to the smectic phase (S_A) and from the smectic to the isotropic phase (I) in some lanthanide complexes is illustrated in Table 1.

The pronounced fanning texture characteristic of the S_A mesophase was observed in a microscope when the samples were heated.

The DSC contains two peaks corresponding to the phase transitions Cr—S and S—I, whose enthalpies

Published in Russian in *Izvestiya Akademii Nauk. Seriya Khimicheskaya,* No. 3, pp. 469—474, March, 2001.

1066-5285/01/5003-488 $25.00

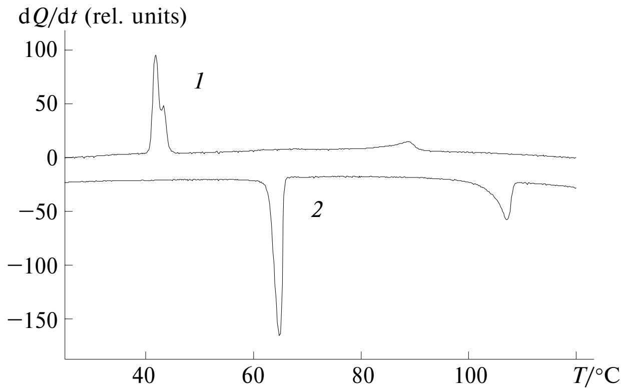

Fig. 1. DSC curves of the mesogenic $L_3Er(C_8H_{17}OSO_3)_3$ complex: *1*, heating and *2*, cooling.

$\Delta H_{Cr-S} \approx 5$ kJ mol^{-1} and $\Delta H_{S-I} \approx 0.5$ kJ mol^{-1} agree well with the presence of the smectic A phase. Note a good convergence of the results of microscopic studies and DSC for the reproduction of several "heating—cooling" cycles, which indicates the stability of the prepared compounds.

The ability to supercooling is a remarkable feature of these compounds. In the same "heating—cooling" cycle, the temperatures of phase transitions can be shifted by 5—25 °C.

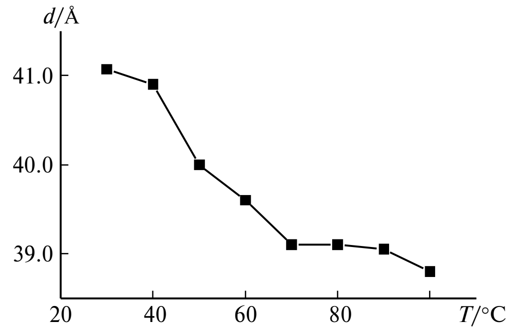

Fig. 2. Temperature plot of the interlayer distance (*d*) in the $L_3Tb(EtOSO_3)_3$ complex.

The temperature plot of the *d* distance between the layers of the molecules in the smectic phase of the $L_3Tb(C_2H_3OSO_3)_3$ complex at room temperature exhibits a peak at 41.1 Å corresponding to the calculated length of the molecule (Fig. 2). The X-ray diffraction curve has several diffuse peaks at 4.2 Å corresponding to the calculated distance between the alkyl chains (Fig. 3, *a*). For other compounds of this series, the interlayer distance increases noticeably with the chain length of the alkyl substituent: $n = 8$, $d = 41.8$ Å; $n = 18$, $d = 43$ Å.

Table 1. Temperatures of phase transitions (T) and mesophase width (ΔT) in some lanthanide complexes $L_3Ln(C_nH_{2n+1}OSO_3)_3$

Ln	n	T/°C		ΔT/°C
		Cr—S$_A$	S$_A$—I	
Tb	2	85	123	38
	3	102	138	36
	4	107	142	35
	5	103	138	35
	6	100	131	31
	7	106	140	34
	8	69	115	19
	9	56	72	16
	10	61	80	19
	12	71	86	15
	13	72	90	18
	15	74	104	30
	18	75	84	9
	19	72	89	17
Er	2	90	129	39
	8	100	113	13
	18	70	90	20

Transition to the smectic A phase (~60 °C) is accompanied by a strong broadening of the peak at 4.2 Å,

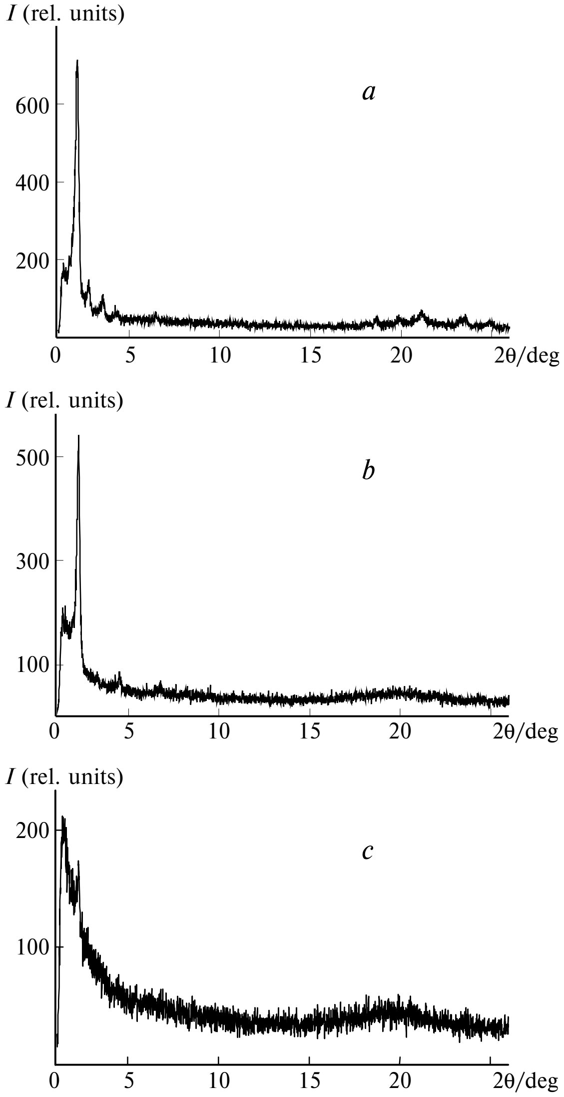

Fig. 3. X-ray diffraction curves for the $L_3Tb(EtOSO_3)_3$ complex at different temperatures: *a*, 30; *b*, 80; and *c*, 100 °C.

which implies the complete disordering of the molecules inside the smectic layers. The shift of the interlayer peak from 41.1 Å to 39 Å (see Fig. 2) indicates the profound rearrangement of the mesophase structure by the inclination of the alkyl chains of the molecules by 20—30° due to the rotation and/or mutual penetration of the alkyl chains (see Fig. 3, *b*). However, the peak begins to shift at lower temperatures than it could be expected from the data of polarization microscopy. This behavior of the mesocomplexes may indicate the existence of a more highly ordered liquid crystalline phase, which is evidenced by two weak reflections at 31.8 and 24.9 Å in the small-angle region at ~20 °C.

Transition to the isotropic phase (~100 °C) is accompanied by a sharp decrease in the intensity and a broadening of both peaks at 4.2 and 33 Å.

After cooling to 25 °C, the peak of the interlayer distance at 41.1 Å (see Fig. 2) and that at 4.2 Å are recovered in the spectrum.

The Tb and Er compounds with different lengths of the hydrocarbon radical possess similar liquid crystalline properties: on heating their melts exhibit in the polarized light the fanning structure typical of the smectic A mesophase. However, the temperature intervals of the existence of the mesophases (ΔT) decrease substantially with an increase in the length of the alkyl substituent in the alkylsulfate group (see Table 1). Nevertheless, in several cases, they are much lower than the corresponding intervals for similar complexes with the NO_3^- anion (for example, for Tb^{III}, T_{Cr} = 96, T_{S_A} = 149 °C).[8]

The influence of the number of carbon atoms in the alkylsulfate fragment on the temperatures of phase transitions of the Tb complexes is presented in Fig. 4. When the chain length of the alkyl fragment in the alkylsulfate ion increases to n = 4, the temperatures of phase transitions increase insignificantly, and then at n = 9 they decrease sharply. Perhaps, this is related to an increase in the mobility and volume of the rotating alkyl chains in the alkylsulfate chain on heating, this results in the loosening of the liquid crystalline system and its faster disordering.

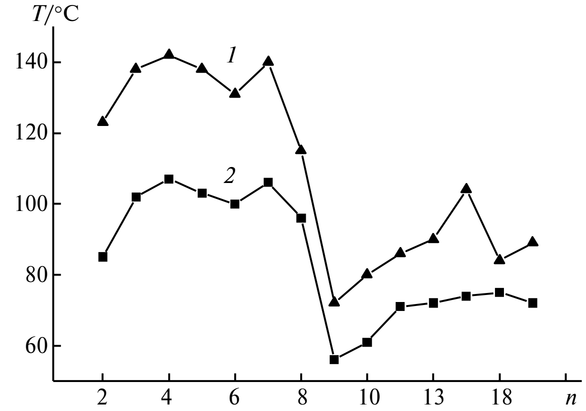

Fig. 4. Temperatures of phase transitions of the alkylsulfate complexes $L_3Tb(C_nH_{2n+1}OSO_3)_3$: *1*, S_A—I transition and *2*, Cr—S_A transition.

The temperatures of the smectic-isotropic transition are maximal at the average length of the alkyl chain (n = 4—7), and at n = 9 the phase transition temperature decreases sharply. With the further elongation of the alkyl chain, the isotropization temperatures increase slowly but do not reach the maximal value at n = 8. No distinct alternation of the clearing-up temperatures for the terbium complexes with this ligand is observed (the corresponding curve is smoothened).

A comparison of the results shows that the temperature of transitions for all alkylsulfates $L_3Tb(C_{15}H_{31}OSO_3)_3$ are lower than that for the nitrate derivative.

The compounds with the radical chain length with n = 8, 9 ($L_3Tb(C_8H_{17}OSO_3)_3$, $L_3Er(C_8H_{17}OSO_3)_3$, $L_3Tb(C_9H_{19}OSO_3)_3$) have the minimal temperatures of phase transitions.

The magnetic properties of the complexes are presented in Table 2. The magnetic moment observed at ~20 °C corresponds to the L_3LnX_3 composition and elemental analysis data.

The orientational behavior of the mesophases in the magnetic field was studied by the photodetection of the X-ray spectra. The cycle of measurements included heating of a capillary filled with the sample to the tempera-

Table 2. Magnetic moment (μ_{eff}) in various phases and magnetic parameters of the mesogenic $L_3Ln(C_nH_{2n+1}OSO_3)_3$ complexes

Ln	n	T_{I-S}	T_{S-Cr}	μ_{eff}/μ_B				$(\chi_{or} - \chi_{iso}) \cdot 10^6$ * /cm^3 mol^{-1}	$\Delta\chi_{min}$**
		°C		Calculation	I	S	Cr		
Tb	2	84	44	9.7	9.64	9.74	9.74	760	−2280
	8	85	45		9.71	9.84	9.84	970	−2910
	10	71	56		9.29	9.44	9.44	1040	−3120
	18	70	55		9.31	9.47	9.47	1125	−3375
Er	2	129	69	9.5	9.19	9.35	9.55	2465	3700
	8	95	71		9.44	9.59	9.74	2085	3130
	18	73	56		9.76	9.79	9.85	670	1000

* All data on the magnetic susceptibility χ correspond to the temperature T_{S-Cr}.

** The sign of $\Delta\chi_{min}$ was determined by the X-ray diffraction data in the oriented mesophases.

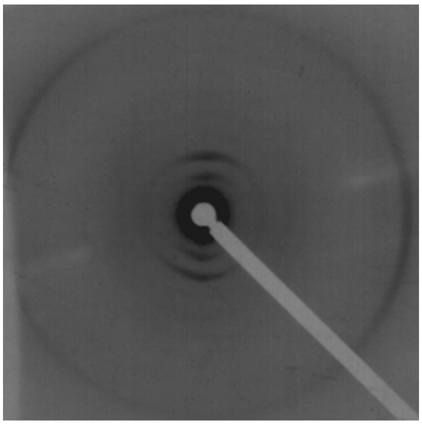

Fig. 5. X-ray diffraction pattern of the $L_3Er(C_8H_{17}OSO_3)_3$ complex in the magnetic field at 80 °C.

ture, which exceeded by several degrees T_{S-I}, and cooling in the magnetic field to the transition to the mesophase. The Er^{III} complexes are oriented by their long axis parallel to the magnetic field (Fig. 5), and the Tb^{III} complexes are perpendicularly oriented. This behavior of the mesocomplexes agrees well with the Bleaney theory of magnetic anisotropy of lanthanides.[11]

Typical curves of the temperature plot of the effective magnetic moment μ_{eff} of the mesogenic $L_3Er(C_8H_{17}OSO_3)_3$ and $L_3Er(EtOSO_3)_3$ complexes are presented in Fig. 6. The cycle of measurements included heating to temperatures several degrees exceeding the transition temperature T_{S-I} and cooling of the sample to ~20 °C. On the first heating in the studied temperature interval, the magnetic moment remained unchanged. On cooling of the sample in the temperature region of the transition of the smectic A phase to the isotropic phase, we observed a noticeable increase in μ_{eff}, which is resulted by the magnetic field-induced orientation of the liquid crystalline sample at which the axis with the maximal magnetic susceptibility is arranged parallel to the field direction. With the further temperature decrease, the magnetic moment continues to increase to a higher value.

In studying the compounds of this class, the Er^{III} complexes were first to exhibit the second noticeable jump of the magnetic moment μ_{eff}(Cr) in the temperature region of the transition of the crystalline to the smectic A phase. This indicates, perhaps, the existence of a more highly ordered liquid crystalline phase, which correlates to the XDA data.

Using the $\chi_{or} - \chi_{iso}$ difference measured at T_{S-Cr} (see Table 2) and XRD data on the orientation of the mesophases, we estimated the minimal molecular magnetic anisotropy $\Delta\chi_{min} = -3(\chi_{or} - \chi_{iso})$ for the Tb^{III} complexes and $\Delta\chi_{min} = 1.5(\chi_{or} - \chi_{iso})$ for the Er^{III} complexes. The increase in the magnetic anisotropy of the Tb^{III} complexes with the elongation of the alkyl counterion chain can be a consequence of a decrease in the mesophase viscosity and/or of an increase in the axial distortion of the complex, which, according to the published data,[13] increases its magnetic anisotropy. A reverse tendency is observed for the Er^{III} compounds with the opposite orientation in the magnetic field.

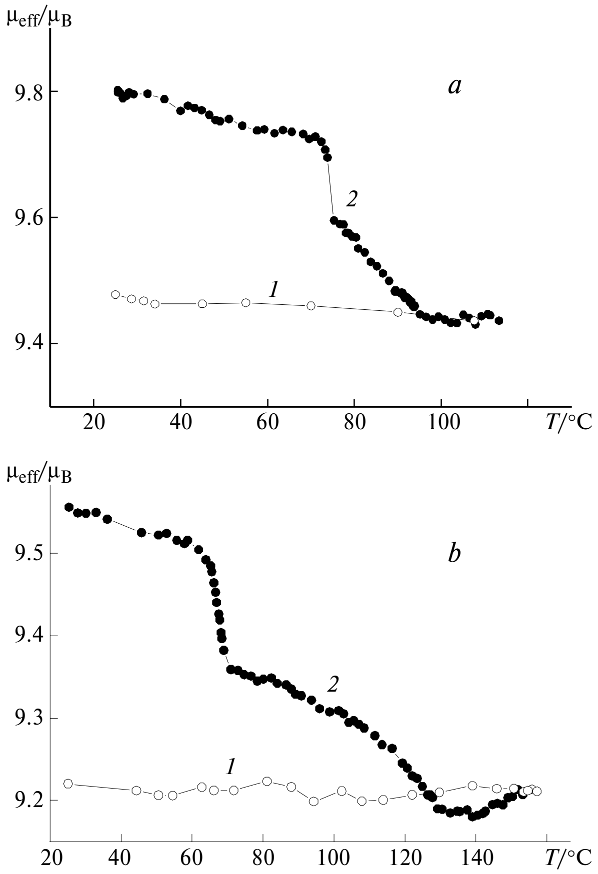

Fig. 6. Temperature plot of the effective magnetic moment (μ_{eff}) of the mesogenic $L_3Er(C_8H_{17}OSO_3)_3$ (*a*) and $L_3Er(EtOSO_3)_3$ (*b*) complexes: *1*, heating and *2*, cooling.

Thus, our study revealed a substantial influence of the chain length of the alkyl fragment on the liquid crystalline properties and orientation in the magnetic field of the mesogenic lanthanide complexes.

Experimental

The temperatures and types of phase transitions were determined on a Perkin Elmer DSC-2C differential scanning calorimeter and a polarization microscope provided with an automated temperature block (accuracy of temperature determination ±0.1 °C). ^{1}H NMR spectra were recorded on a Varian UNITY-300 spectrometer (300 MHz) in $CDCl_3$ using Me_4Si as an internal standard.

X-ray diffraction curves were recorded by the photomethod in the magnetic field with 0.8 T and using a STOE STADI 2 diffractometer (the setup was described in more detail in Ref. 14).

The magnetic susceptibility was measured by the Faraday method within the 20—150 °C temperature interval at a magnetic field intensity of 15 kG on a setup described in Ref. 12.

The magnetic susceptibility at ~20 °C was used to calculate the effective magnetic moment (μ_{eff}):

$$\mu_{\text{eff}}^2 = [3kT(\chi_M - \chi_d)]/(g_i N_A) \approx 8T(\chi_M - \chi_d),$$

where k is the Boltzmann constant, T is the temperature, χ_M is the molar magnetic susceptibility, χ_d is the diamagnetic correction calculated using the Pascal scheme, and g_i is the Lande g factor. The measurements of the magnetic susceptibility at different temperatures were processed and the magnetic parameters of the compounds were calculated by the previously described method.[15]

The L ligand was synthesized by the alkylation of 2,4-dioxybenzaldehyde using a known procedure.[3]

The structure of the L ligand was confirmed by the data of ^{1}H NMR, δ: 0.88 (t, 6 H, Me); 1.10—1.50 (m, 44 H, CH_2); 1.67 (m, 2 H, $NCH_2C\underline{H}_2$); 1.77 (m, 2 H, $OCH_2C\underline{H}_2$); 3.57 (t, 2 H, NCH_2); 3.95 (t, 2 H, $OC\underline{H}_2$); 6.31 (dd, 1 H, Ph, J_o = 2.5 Hz); 6.35 (d, 1 H, Ph, J_o = 8.5 Hz, J_m = 2.5 Hz); 7.05 (d, 1 H, Ph, J_o = 8.5 Hz); 8.08 (s, 1 H, CH=N); 14.09 (s, 1 H, OH). $C_{35}H_{63}NO_2$.

The composition of complexes was found by elemental analysis (Table 3) and comparison of the measured and calculated magnetic moments at ~20 °C.

Sodium ethylsulfate. EtOH (3.5 mL, 45 mmol) was added to conc. H_2SO_4 (3.5 mL, 65 mmol) with stirring at ~20 °C. The mixture was stored for 5 min at 50 °C and poured in ice-cold water (50 mL). The resulting solution was neutralized with powdered $BaCO_3$ to pH 7. The precipitate of $BaSO_4$ was filtered off, and the filtrate was evaporated. Dried barium ethylsulfate (4.5 g, 10^{-2} mol) was dissolved in water, and $Na_2CO_3 \cdot 10H_2O$ (5.72 g, 20 mmol) was added to the solution. The precipitated $BaCO_3$ was filtered off. The solution was evaporated, and the formed sodium ethylsulfate was dried above P_2O_5. Sodium isopropyl-, butyl-, and amylsulfates were prepared similarly.

Sodium hexylsulfate. $C_6H_{13}OH$ (4.8 mL, 45 mmol) was added to conc. H_2SO_4 (5 mL, 65 mmol) with stirring at ~20 °C. The solution became lemon-yellow. The reaction mixture was stirred for 30 min and poured in ice-cold water (50 mL). The resulting solution was neutralized with Na_2CO_3 to pH 7 and salted out with a 10% solution of NaCl. The prepared sodium

Table 3. Elemental analysis data for the lanthanide complexes with the alkylsulfate counterion

Formula	Molecular weight	Found/Calculated (%)			Molecular formula
		C	H	N	
$L_3Tb(EtOSO_3)_3$	2123.94	62.79 62.76	9.65 9.68	1.97 1.98	$C_{111}H_{204}N_3O_{18}S_3Tb$
$L_3Tb(C_3H_7OSO_3)_3$	2166.01	63.26 63.21	9.72 9.77	1.92 1.94	$C_{114}H_{210}N_3O_{18}S_3Tb$
$L_3Tb(C_4H_9OSO_3)_3$	2208.09	63.67 63.64	9.82 9.86	1.89 1.90	$C_{117}H_{216}N_3O_{18}S_3Tb$
$L_3Tb(C_5H_{11}OSO_3)_3$	2250.17	64.07 64.05	9.90 9.94	1.85 1.87	$C_{120}H_{222}N_3O_{18}S_3Tb$
$L_3Tb(C_6H_{11}OSO_3)_3$	2292.25	64.52 64.45	10.00 10.02	1.81 1.83	$C_{123}H_{228}N_3O_{18}S_3Tb$
$L_3Tb(C_7H_{15}OSO_3)_3$	2334.33	64.78 64.83	10.05 10.10	1.78 1.80	$C_{126}H_{234}N_3O_{18}S_3Tb$
$L_3Tb(C_8H_{17}OSO_3)_3$	2376.41	65.20 65.19	10.15 10.18	1.76 1.77	$C_{129}H_{240}N_3O_{18}S_3Tb$
$L_3Tb(C_9H_{19}OSO_3)_3$	2418.49	65.49 65.55	10.19 10.25	1.73 1.74	$C_{132}H_{246}N_3O_{18}S_3Tb$
$L_3Tb(C_{10}H_{21}OSO_3)_3$	2460.57	65.78 65.89	10.27 10.32	1.69 1.71	$C_{135}H_{252}N_3O_{18}S_3Tb$
$L_3Tb(C_{12}H_{25}OSO_3)_3$	2544.73	66.48 66.55	10.43 10.46	1.63 1.65	$C_{141}H_{264}N_3O_{18}S_3Tb$
$L_3Tb(C_{13}H_{27}OSO_3)_3$	2586.81	66.82 66.86	10.49 10.52	1.59 1.62	$C_{144}H_{270}N_3O_{18}S_3Tb$
$L_3Tb(C_{15}H_{31}OSO_3)_3$	2670.97	67.42 67.45	10.59 10.64	1.55 1.57	$C_{150}H_{282}N_3O_{18}S_3Tb$
$L_3Tb(C_{18}H_{37}OSO_3)_3$	2797.21	68.17 68.27	10.74 10.81	1.49 1.50	$C_{159}H_{300}N_3O_{18}S_3Tb$
$L_3Tb(C_{19}H_{39}OSO_3)_3$	2839.29	68.46 68.52	10.80 10.86	1.45 1.47	$C_{162}H_{306}N_3O_{18}S_3Tb$
$L_3Er(EtOSO_3)_3$	2132.27	62.50 62.53	9.59 9.64	1.95 1.97	$C_{111}H_{204}ErN_3O_{18}S_3$
$L_3Er(C_8H_{17}OSO_3)_3$	2384.75	64.88 64.97	10.11 10.14	1.72 1.76	$C_{129}H_{240}ErN_3O_{18}S_3$
$L_3Er(C_{18}H_{37}OSO_3)_3$	2763.47	67.59 67.80	10.62 10.72	1.49 1.52	$C_{156}H_{294}ErN_3O_{18}S_3$

hexylsulfate was filtered off and recrystallized in hot EtOH. The filtrate was evaporated and dried above P_2O_5. Sodium heptyl-, octyl-, nonyl-, dodecylsulfates were prepared similarly.

Tb^{III} ethylsulfate. Equimolar amounts of alcohol solutions of $TbCl_3$ (0.17 g, 0.64 mmol) and ethylsulfate (0.31 g, 1.9 mmol) were mixed at ~20 °C. The precipitated NaCl was filtered off, the filtrate was evaporated, and the residue was dried *in vacuo* above P_2O_5. The product was obtained in 92% yield (3 g). Found (%): C, 12.95; H, 2.71. $C_6H_{15}O_{12}S_3Tb$. Calculated (%): C, 12.90; H, 2.69. Isopropyl-, butyl-, amyl-, hexyl-, heptyl-, octyl-, nonyl-, and decylsulfates were prepared similarly.

Tb^{III} dodecylsulfate. Equimolar amounts of aqueous solutions of $Tb(NO_3)_3 \cdot 6H_2O$ (0.3 g, 0.65 mmol) and sodium dodecylsulfate (0.6 g, 1.8 mmol) were mixed at ~20 °C. Then the solution was heating to boiling. The white precipitate of Tb^{III} dodecylsulfate was formed. The precipitate was filtered off and dried. The product was obtained in 92% yield (1 g). Found (%): C, 45.27; H, 7.91. $C_{12}H_{75}O_{12}S_3Tb$. Calculated (%): C, 45.17; H, 7.95.

Preparation of $L_3Tb(C_{12}H_{25}OSO_3)_3$ complex. A solution of the L ligand (0.42 g, 0.75 mmol) in EtOH was gradually added dropwise to an alcohol solution of terbium dodecylsulfate (0.23 g, 0.25 mmol) at 50 °C. The solution was left for 2 h, and a yellow precipitate was formed. The precipitate was filtered off, twice washed with EtOH, and dried *in vacuo* above P_2O_5. The yield of the product was 0.52 g (80%). Found (%): C, 66.48; H, 10.43, N, 1.63. $C_{141}H_{264}N_3O_{18}S_3Tb$. Calculated (%): C, 66.55; H, 10.46, N, 1.65.

This work was financially supported by the Russian Foundation for Basic Research (Project No. 99-03-32716), the German Scientific Society DFG (Grant 436RUS/113/401), and the Volkswagen Foundation VW-Stiftung (Grant I/72818).

References

1. D. W. Bruce, *Inorganic Materials*, Eds. D. W. Bruce and D. O. Hare, Wiley, Chichester, 1992, 405.
2. S. A. Hadson and P. M. Maitlis, *Chem. Rev.*, 1993, **93**, 861.
3. Yu. G. Galyametdinov, G. I. Ivanova, and I. V. Ovchinnikov, *Izv. Akad. Nauk, Ser. Khim.*, 1991, 1232 [*Bull. Acad. Sci. USSR*, *Div. Chem. Sci.*, 1991, **40**, 1109 (Engl. Transl.)].
4. Yu. Galyametdinov, M. Athanassopoulou, S. Hiller, L. Beresnev, M. Schweissguth, and W. Haase, *Mol. Cryst. Liq. Cryst.*, 1995, 261.
5. A. V. Prosvirin, Yu. G. Galyametdinov, G. I. Ivanova, and O. N. Kadkin, *Izv. Akad. Nauk, Ser. Khim.*, 1994, 1003 [*Russ. Chem. Bull.*, 1994, **43**, 938 (Engl. Transl.)].
6. Yu. G. Galyametdinov, I. V. Ovchinnikov, and A. V. Prosvirin, *Izv. Akad. Nauk, Ser. Khim.*, 1995, 787 [*Russ. Chem. Bull.*, 1995, **44**, 768 (Engl. Transl.)].
7. Yu. G. Galyametdinov, M. Atanassopoulo, W. Haase, and I. V. Ovchinnikov, *Koord. Khim.*, 1995, **21**, 751 [*Russ. J. Coord. Chem.*, 1995, **21** (Engl. Transl.)].
8. Yu. G. Galyametdinov, M. Athanassopoulou, K. Griesar, O. A. Kharitonova, E. Soto-Bustamante, L. M. Tinchurina, I. V. Ovchinnikov, and W. Haase, *Chem. Mat.*, 1996, 922.
9. Yu. G. Galyametdinov, G. I. Ivanova, I. V. Ovchinnikov, A. N. Prosvirin, D. Guillon, B. Heinrich, D. A. Dunmur, and D. W. Bruce, *Liquid Cryst.*, 1996, **20**, 831.
10. Yu. G. Galyametdinov, G. I. Ivanova, I. V. Ovchinnikov, K. Binnemans, and D. Bruce, *Izv. Akad. Nauk, Ser. Khim.*, 1999, 387 [*Russ. Chem. Bull.*, 1999, **48**, 385 (Engl. Transl.)].
11. A. Abragam and B. Bleaney, *Electron Paramagnetic Resonance of Transitions*, Clarendon Press, Oxford, 1970.
12. L. Merz and W. Haase, *J. Chem. Soc.*, *Dalton Trans.*, 1980, 875.
13. S. G. Vul′fson, *Molekulyarnaya Magnetokhimiya* [*Molecular Magnetochemistry*], Nauka, Moscow, 1991, 261 pp. (in Russian).
14. Z. X. Fan and W. Haase, *J. Chem. Phys.*, 1991, **95**, 6066.
15. K. Binnemans, Yu. Galyametdinov, R. Van Deun, D. Bruce, S. Collinson, A. Polishchuk, I. Bikchantaev, W. Haase, A. Prosvirin, L. Tinchurina, I. Litvinov, A. Rakhmatullin, K. Uytterhoeven, and L. Meervelt, *J. Am. Chem. Soc.*, 2000, **122**, 433.

Received April 7, 2000